An assessment of combustion dynamics in a low-NO_x, second-generation swirl-venturi lean direct injection combustion concept

K.M. Tacina[1], C.T. Chang[1], P. Lee[2], H. Mongia[3⋆]

[1]Engine Combustion Branch, NASA Glenn Research Center, Cleveland, Ohio
[2]Woodward FST, Inc., Zeeland, MI
[3]Purdue University West Layfette, IN

Abstract

Dynamic pressure measurements were taken during flametube emissions testing of three second-generation swirl-venturi lean direct injection (SV-LDI) combustor configurations. These measurements show that combustion dynamics were typically small. However, a small number of points showed high combustion dynamics, with peak-to-peak dynamic pressure fluctuations above 0.5 psi. High combustion dynamics occurred at low inlet temperatures in all three SV-LDI configurations, so combustion dynamics were explored further at low temperature conditions. A point with greater than 1.5 psi peak-to-peak dynamic pressure fluctuations was identified at an inlet temperature of 450°F, a pressure of 100 psia, an air pressure drop of 3%, and an overall equivalence ratio of 0.35. This is an off-design condition: the temperature and pressure are typical of 7% power conditions, but the equivalence ratio is high. At this condition, the combustion dynamics depended strongly on the fuel staging. Combustion dynamics could be reduced significantly without changing the overall equivalence ratio by shifting the fuel distribution between stages. Shifting the fuel distribution also decreased NO_x emissions.

Keywords: combustion, combustion dynamics, low emissions combustors

I. Introduction

One major focus of NASA's aeronautics programs is to reduce emissions of the oxides of nitrogen, NO_x. NO_x emissions can be reduced by burning fuel-lean throughout: all combustion air enters through the dome[1,2,3,4,5]. However, fuel-lean gas turbine combustors have been susceptible to combustion dynamics and instabilities when used for ground-based power generation[6,7,8]; fuel-lean combustors have also been shown to be susceptible when used in aero-engines[9,10]. Therefore, to aide in screening low-emissions aircraft combustor concepts for combustion dynamics, NASA routinely measures dynamic pressure fluctuations.

Although dynamic pressure fluctuations can indicate that combustion dynamics are becoming problematic, they give limited insight into their source. To gain insight into the source of the combustion dynamics, we must look at acoustic theory as well as the literature on unsteady combustion and combustion dynamics.

From basic acoustic theory, a given combustor or flametube geometry will have characteristic natural frequencies where acoustics can be magnified, i.e., resonance frequencies. These natural acoustic modes can be excited by unsteady heat release. The acoustics and unsteady heat release can excite natural hydrodynamic instabilities and interact with existing unsteady features in the fluid flow[11,12,13].

Unsteady features are prominent in gas turbine combustion. One set of unsteady features is caused by the mechanism used to anchor and stabilize the flame and to promote fuel-air mixing: swirling flow, i.e., flow with azimuthal rotation. When the swirl is high enough, a central recirculation zone (CRZ) will form[14,15]. Often associated with this central recirculation zone is a precessing vortex core (PVC),[11,12,16] in which the axis of rotation of the swirling flow is itself rotating around the geometric center of the flow field. In addition to the PVC and other unsteady structures associated with swirling flows, the edges of shear layers may exhibit the Kelvin-Helmholtz instability. Finally, there may be additional unsteady features associated with the fuel spray.

Multiple unsteady features can be expected in the low emissions combustor concept tested here. The concept is a second-generation swirl-venturi (SV) lean direct injection (LDI) combustion concept. In LDI, multiple small fuel-air mixers replace one traditionally-sized fuel-air mixer. Each fuel-air mixer can potentially have its own central recirculation zone

⋆Other authors: D. P. Podboy[1] and B. Dam[2]

and PVC; the Kelvin-Helmholtz instability can form at the edge of each shear layer.

Each of the fuel-air mixers in LDI is relatively simple. As shown in Fig. 1, a single swirl-venturi LDI (SV-LDI) fuel-air mixer consists of a fuel injector and an air passage with an axial air swirler followed by a converging-diverging venturi section. The fuel injector is inserted through the center of the air swirler, with the tip typically located at the venturi throat.

In the first-generation SV-LDI configurations, each fuel-air mixer was identical or nearly-identical, with only two variations. First, the swirler vane angles could be varied; typical vane angles were 45° or 60°. Second, the fuel-air mixers were split into multiple fuel circuits to investigate fuel staging[3,17,18].

In second-generation SV-LDI, the fuel-air mixer design has three additional variations. First, the size of each fuel-air mixer can be small or large. Second, the fuel-air mixers can be recessed from the dome or not recessed. Third, the type of fuel injector can be either simplex (like all first-generation LDI fuel-air mixers) or airblast.

The type of fuel injector will effect the air flow. As illustrated in Figure 1, a fuel-air mixer with an airblast fuel injector will have two air swirlers, the inner air swirler and the outer air swirler; a fuel-air mixer with a simplex fuel injector will have only a single (outer) air swirler.

Second-generation SV-LDI configurations have four fuel circuits, called stages: a pilot stage and three main stages, main-1, main-2, and main-3. Within each stage, all fuel-air mixers are identical. The pilot stage has a single large fuel-air mixer and each main stage has four small fuel-air mixers.

Since the fuel-air mixer design can vary for each stage, each stage may have different unsteady features and different interactions with the acoustic modes. Due to these differences, shifting the fuel from one stage to another may change the interaction between the unsteady heat release and the acoustics even if overall fuel flow rate does not change. In other words, changing the fuel staging may change the combustion dynamics. The differences may also allow combustion dynamics to be associated with a given fuel-air mixer design. Therefore, changing the fuel staging has the potential to reduce combustion dynamics.

The purpose of this testing was (1) to determine if combustion dynamics were typically strong, (2) to identify points with strong combustion dynamics, (3) to determine if changing fuel staging would change the combustion dynamics without adversely effecting gaseous emissions and (4) to identify, if possible, the source of the combustion dynamics.

II. Experimental Facilities and Hardware

A. LDI Hardware

Three second-generation SV-LDI configurations were tested. These configurations are named for the number of fuel-air mixers that are recessed: for the flat dome configuration, no fuel-air mixers are recessed; for the 5-recess, the pilot and the four main-1 fuel-air mixers are recessed; and for the 9-recess, the pilot, the four main-1, and the four main-2 fuel-air mixers are recessed. These configurations are shown in Figure 2, with each stage labeled. The fuel injector types and swirler angles for each stage of each configuration are given in Table 1.

B. Flametube Facility

These tests were done in the CE-5 intermediate pressure combustion facility flametube at NASA Glenn Research Center. A sketch of a flametube is shown in Fig. 3. The flametube has a cast ceramic liner. This facility can supply nonvitiated air preheated to 1200 F at pressures up to 275 psia. The test rig supports up to four fuel circuits.

The geometry of the flametube and the upstream piping will determine the acoustic modes. The flametube test section was configured to have a 4.5-in × 4.5-in square cross section. Starting from the dome, the length of the flametube is approximately 34-in. At 34-in, there is a sudden expansion into a larger pipe, and at 42-in downstream of the dome, there is the first water spray bar. The upstream piping has a 12.5-in inner diameter; there are flow straighteners 55-in and 59-in upstream of the dome and an elbow 85-in upstream.

C. Steady-State Data Acquisition and Processing

Steady-state data was acquired at a rate of 1 Hz using the NASA Glenn ESCORT real-time data acquisition system. It recorded facility conditions such as temperature and pressure as well as gaseous emissions.

Gaseous emissions were measured using a 5-hole probe connected to a gas bench, which followed the SAE ARP-1255D[19] standard. Post-processing followed the SAE ARP-1533B[20] standard. Adiabatic flame temperatures are calculated using the Chemical Equilibrium for Applications (CEA) equilibrium code[21,22].

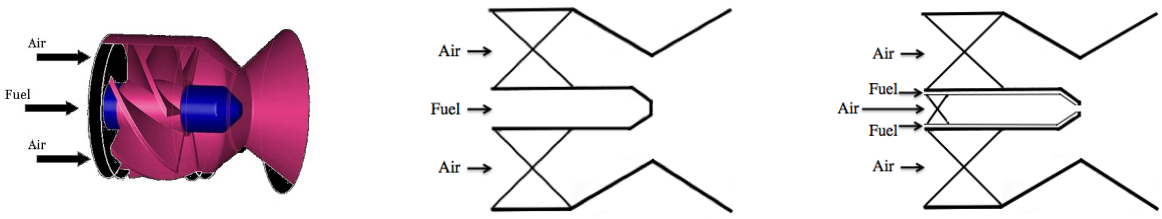

(a) (b) (c)

Figure 1. Illustrations of a single SV-LDI fuel-air mixer: (a) isometric drawing with a simplex fuel injector, (b) sketch with a simplex fuel injector, (c) sketch with an airblast fuel injector.

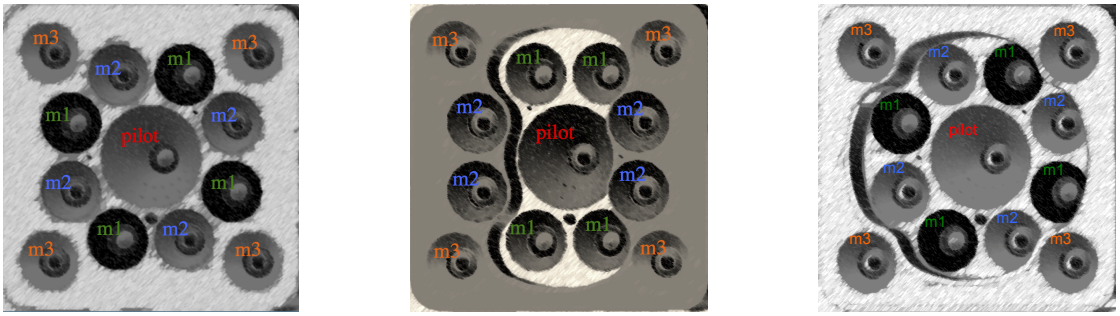

(a) (b) (c)

Figure 2. Second generation SV-LDI hardware: (a) flat dome, (b) 5-recess, and (c) 9-recess configurations.

D. Dynamic Pressure Measurements and Processing

Dynamic pressure fluctuations were recorded using a Data Translation DT9841-sb high speed data acquisition system. The data acquisition rate and recording time varied; typically, they were 20 kHz and 30-sec, respectively.

The dynamic pressure fluctuations were measured upstream (p'_3) and downstream of the dome (p'_4). The pressure transducers were PCB model 112A22. These pressure transducers were designed for room temperature measurements, so they were standoff-mounted 3-ft away from the flametube in 0.25-in stainless steel tubing (i.d.: 0.180-in). Each pressure transducer was followed by a 125-ft semi-infinite loop tail to reduce resonances from acoustic wave reflection.

Unfortunately, in addition to reducing resonances, the standoff-mounting of the pressure transducers also introduces attenuation due to viscous dissipation[23,24,25]. The calculated effect of the resonances and attenuation is shown in Figure 4.

The measured pressure spectrum was corrected for these effects following Samuelson[25]. In addition to correcting for resonances and attenuation, the signal was post-processed to reduce noise using an averaging technique.

III. Results and Discussion

Emissions results for the first two configurations were reported previously[26]; the major result was that these configurations reduced the NO_x emissions by more than 75% with respect to the CAEP/6 standards. Emissions results from the third configuration will be reported later. This rest of this paper focuses on combustion dynamics results.

A. Exploration of Combustion Dynamics

At almost all points tested, combustion dynamics were small: The pressure fluctuations were less than 0.5 psi peak-to-peak. However, for a small number of conditions, there were significant combustion dynamics. The conditions with high combustion dynamics are listed in Table 2.

Since all three configurations had significant combustion dynamics at low inlet temperatures and since combustion instabilities were least likely to damage the combustor and flametube hardware at low temperatures and pressures, an inlet temperature of 450°F and a pressure of 100 psia was chosen for further combustion dynamics investigation. This roughly corresponds to 7% engine power. This investigation was done with the last combustor configura-

Table 1. Second Generation SV-LDI configurations. For each stage, the table gives the type of fuel injector and the air swirler angle(s). (OAS: outer air swirler, IAS: inner air swirler, cw=clockwise, ccw=counterclockwise)

Configuration	Pilot Injector	Pilot Swirler	Main 1 Injector	Main 1 Swirler	Main 2 Injector	Main 2 Swirler	Main 3 Injector	Main 3 Swirler
Flat Dome	Simplex	55° ccw	Simplex	45° ccw	Airblast	IAS: 45° cw OAS: 45° cw	Airblast	IAS: 45° cw OAS: 45° cw
5-Recess	Airblast	IAS: 57° cw OAS: 57° ccw	Simplex	45° cw	Airblast	IAS: 45° cw OAS: 45° ccw	Airblast	IAS: 45° cw OAS: 45° ccw
9-Recess	Airblast	IAS:57° cw OAS: 57° ccw	Simplex	45° ccw	Airblast	IAS: 45° cw OAS: 45° cw	Airblast	IAS: 45° cw OAS: 45° cw

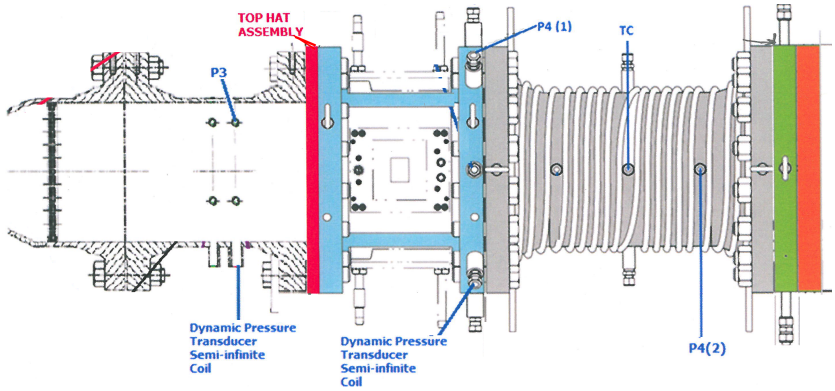

Figure 3. The flametube used for testing the second generation SV-LDI configurations.

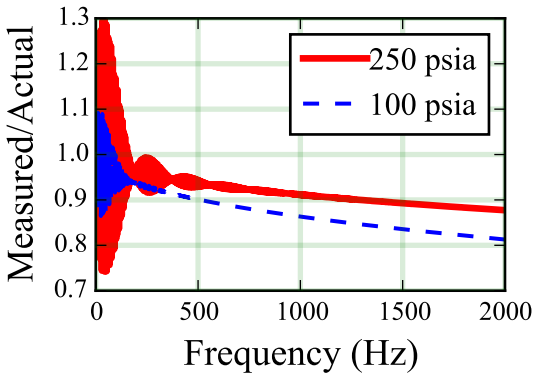

Figure 4. Ratio of measured-to-actual dynamic pressure signal as a function of frequency for combustor pressures of 250 and 100 psia.

tion tested, the 9-recess configuration. The purpose of the investigation was two-fold: (1) to determine if changing the fuel staging decreased the combustion dynamics and (2) to determine, if possible, the source of the combustion dynamics.

Table 2. Conditions with peak-to-peak combustion dynamics greater than 0.5 psia. 7% power conditions refers to inlet temperature T_3 from 400-600°F and pressure p_3 on the order of 100 psia. High T3 refers to inlet temperatures above 900 F.

Configuration	Conditions with large dynamics
Flat dome	$T_3 = 500$°F, $p_3 = 150$ psia, $\phi \geq 0.6$ High T_3, ϕ near 0.3
5-recess	7% power, $\phi \geq 0.26$
9-recess	7%, $\phi \geq 0.25$ 30% power, $\phi > 0.35$ High T_3, ϕ near 0.3

B. Effect of fuel staging at 7% power conditions

Significant combustion dynamics were identified at an air pressure drop 3% and overall equivalence ratio of 0.35 with only the pilot and main-1 (simplex) stages fueled. An equivalence ratio of 0.35 is high for 7% power conditions; this equivalence ratio was chosen because the combustion dynamics were found to be intermittent at lower equivalence ratios.

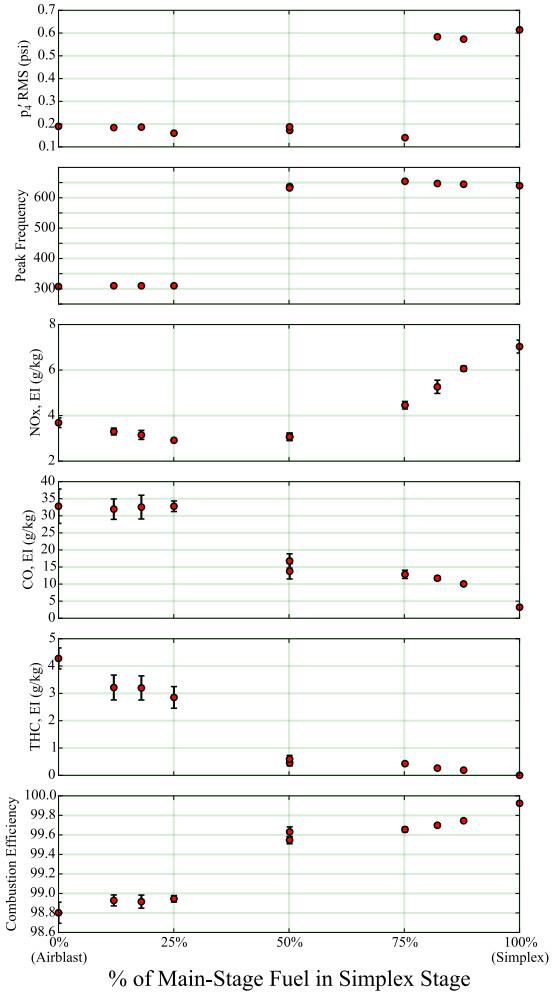

Figure 5. Effect of main fuel staging on combustion dynamics and gaseous emissions at 450°F, 100 psia, and an overall equivalence ratio of 0.35. The pilot fuel flow is kept fixed and the main fuel is split between the simplex main-1 stage and the airblast main-2 stage.

At these conditions, the calculated acoustic mode frequencies are as follows. The transverse half-wave frequency for the flametube cross-section in 3110 Hz. Based on the distance from the dome to the sudden expansion, the longitudinal quarter-wave frequency of the flametube is 210 Hz. Based on the distance to the first flow straightener, the longitudinal quarter-wave frequency of the upstream piping is 80 Hz.

1. *Effect of fuel staging on combustion dynamics*

Changing the fuel staging was found to decrease the combustion dynamics. Keeping both the overall fuel flow and the fuel flow to the pilot stage constant, the main-2 (airblast) stage was turned on and fuel was shifted from the main-1 stage to the main-2 stage. (Main stage 3 stayed off.) This fuel shift decreased the dynamic pressure fluctuation p'_4 significantly; shifting all of the main stage fuel to the main-2 airblast stage decreased the rms value by a factor of 3, as shown in Figure 5.

Changing the fuel staging also helped to tentatively identify the source of the combustion dynamics because changing the fuel staging changed not only the magnitude of the combustion dynamics but also the location of the peak in the frequency spectrum. As Figure 5 shows, when the main stage fuel was shifted from the main-1 simplex stage to the main-2 airblast stage, the location of the peak in the frequency spectrum shifted from near 650 Hz to near 300 Hz. This shift in peak frequency allows the peak near 650 Hz to be tentatively attributed to the main-1 simplex stage and the peak near 300 Hz to be tentatively attributed to the main-2 airblast stage.

To further explore this frequency-peak identification, the time series and the frequency spectrum are examined in more detail in Figures 6–8. First, the frequency spectrum near 650 Hz is examined. The near-650 Hz frequency component is dominant when all of the main stage fuel is in the simplex main-1 stage: This component can easily by picked out by eye in a time series plot and is an order of magnitude greater than than all other frequency components[1], as shown in the top plots of Figure 6. As main stage fuel is shifted away from the simplex main-1 stage, the magnitude of the near-650 Hz peak diminishes; this can best be seen in Figure 7 and 8. At and above 82% simplex, this drop in magnitude is gradual and the near-650 Hz component is still dominant. However, between 82% and 75% main stage fuel in the simplex stage, the magnitude of the near-650 Hz component drops sharply and this frequency becomes much harder to pick out by eye in the time series plots. As the main fuel in the simplex stage drops below 50%, the near-650 Hz component of frequency is no longer the largest component; instead, the largest component shifts to near-300 Hz. However, the near-650 Hz frequency component remains significant: Even when the simplex main-1 stage is unfueled, the magnitude of the near-650 Hz frequency component is roughly half that of the maximum frequency component, as can be seen by comparing the top and bottom plots in Figure 8. These results strongly suggest that the near-650 Hz component is indeed associated with the

[1]Except for a low-frequency component around 0.1 Hz, which may be associated with the facility control system. For this and all further discussions, the very low frequency components are neglected; this includes all frequency components below 2.1 Hz, which is the lowest frequency that can be resolved when the dynamic pressure signal is processed as described in section II.D.

main-1 simplex stage. Furthermore, since the near-650 Hz component persists even when no fuel is flowing to this stage, the near-650 Hz component seems to be caused by air flow, not fuel flow, although it is amplified by combustion.

Ideally, LES or optical diagnostics would provide insight into the source of the near-650 Hz frequency component. Unfortunately, neither LES nor high-speed optical diagnostics are available. However, we can hypothesize a source of the near-650 Hz component using steady-state RANS CFD and the literature. Although no CFD is publicly available for the 9-recess configuration tested here, RANS CFD is available for the flat dome configuration[27]. The RANS results show a central recirculation zone downstream of each of the main-1 simplex fuel-air mixers. A central recirculation zone strongly indicates that a PVC is present[16]. Thus, a PVC may be a direct or indirect cause of the near-650 frequency component.

Note that this does not necessarily mean that the PVC frequency is 650 Hz. Instead, even if it is caused by the PVC, the 650 Hz frequency may be the difference in frequency between the PVC and an acoustic mode or some other unsteady structure; in other words, 650 Hz may be a beat frequency.

Just as the near-650 Hz peak in the frequency spectrum was attributed to the simplex main-1 stage, the near-300 Hz peak in the frequency spectrum was tentatively attributed to the airblast main-2 stage. This attribution is supported by the more detailed analysis of the frequency and time series in Figures 6–8; these figures show that increasing the airblast main-2 stage from 50% of the main stage fuel fuel ("50% simplex") to 75% ("25% simplex") more than doubles the magnitude of the near-300 Hz frequency component. This attribution is also supported by the more complex shape of the frequency spectrum between 200 and 400 Hz. As shown in Figure 7, the local frequency has 5 local peaks from 200-400 Hz. A complex frequency spectrum is consistent with an airblast fuel-air mixer because the interaction between shear layers and possibly PVCs caused by multiple air swirlers would lead to a more complex frequency spectrum. The airblast main-2 stage has two air swirlers — an inner air swirler and an outer air swirler — whereas the simplex main-1 stage has only a single (outer) air swirler. (Compare the air paths of the fuel-air mixers with simplex and airblast fuel injectors in Figure 1.)

A careful examination of the 200-400 Hz frequency spectrum in Figure 7 also suggest the source of the near-300 Hz frequency component: the air flow. This frequency component is present even when the airblast main-2 stage is unfueled ("100% simplex"). In addition, the comparatively complex frequency spectrum between 200 and 400 Hz retains its basic shape regardless of the fuel flow to the airblast main-2 stage: all 5 local frequency peaks remain at the same frequency as the main stage fuel is shifted from all simplex to all airblast. This can best be seen in the lower left plot in Figure 7. Although combustion amplifies the near-300 Hz frequency component, its cause seems to be the air flow.

2. Effect of fuel staging on gaseous emissions

Although combustion dynamics is the focus of this study, gaseous emissions remain critical. In this study, the gas bench measured emissions of NO_x, carbon monoxide (CO), and total hydrocarbons (THC). Note that the NO_x emissions will be higher than typical for a 7% power condition because this combustion dynamics study was done at an off-design point with a higher fuel-air ratio.

Despite the off-design conditions, this study compares the emissions of the simplex main-1 stage and the airblast main-2 stage. If both main-1 and main-2 had similar emissions, the emissions in Figure 6 would be symmetric around 50% main stage fuel to the simplex main-1 stage. This is not the case. Instead, the simplex main-1 stage produces more NO_x but less CO and THC than the airblast main-2 stage. As percentage of main stage fuel in the simplex stage increases above 50%, NO_x emissions increase and CO and THC emissions continuously decrease. The decrease in CO and THC emissions causes the combustion efficiency to increase from 99.6% to 99.9%. In contrast, as the percentage of main stage fuel in the airblast stage increases above 50% ("<50% simplex"), the NO_x first decreases slightly and then gradually increases. However, the CO and THC immediately jump up; the CO than remains at a constant level while the THC continues to increase, causing the combustion efficiency to drop from 99.6% to a still-acceptable (at 7% power) 98.8%.

IV. Conclusions

Dynamic pressure measurements were taken during emissions testing of three second-generation swirl-venturi lean direct injection (SV-LDI) configurations. These measurements show that combustion dynamics were typically small. However, a small number of points showed high combustion dynamics, with peak-to-peak dynamic pressure fluctuations above 0.5 psi. High combustion dynamics occurred at low inlet temperature in all three configurations, so combustion dynamics were explored further at low temperature conditions. A point with larger than 1.5 psi peak-to-

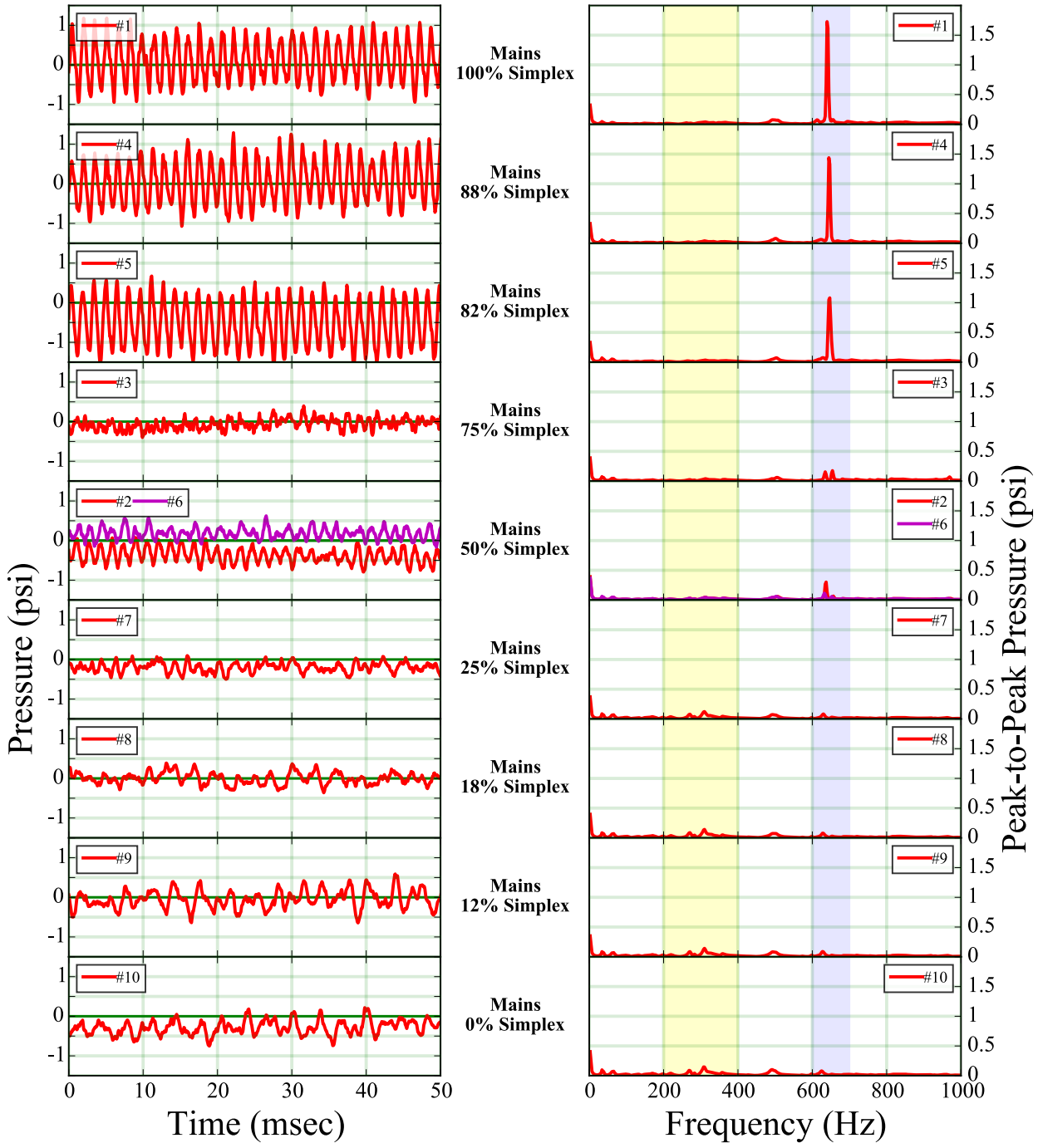

Figure 6. Effect of fuel staging on p'_4: Time series (left) and pressure spectrum (right) as the main stage fuel is shifted from stages main-1 (simplex) to main-2 (airblast). The conditions are the same of those of Figure 5. The number in the legend indicates the order in which the data was taken. There was one repeat, at the 50% simplex case. The highlighting indicates the parts of the frequency spectrum examined in more detail in Figures 7 and 8.

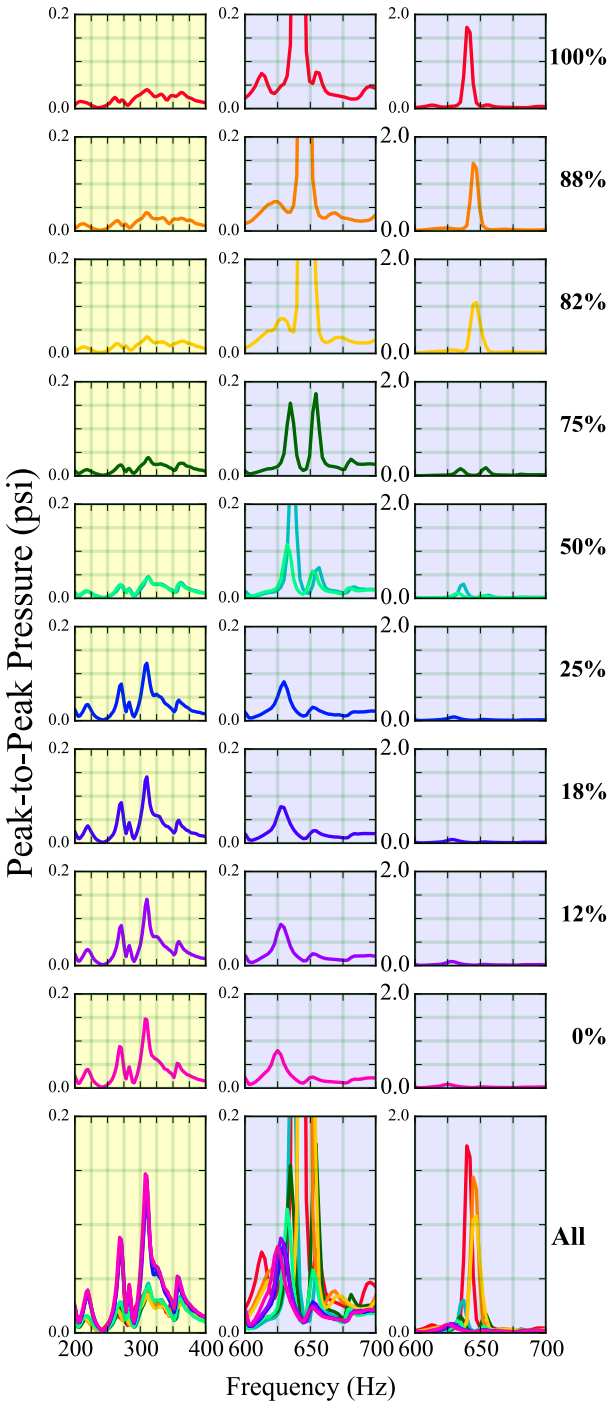

Figure 7. Pressure spectrum of p'_4 showing the regions highlighted in the frequency spectrum plots in Figure 6. The label on the right indicates the percentage of main fuel flow going to the main-1 simplex stage; at 100%, all main fuel flow goes to the simplex main-1 stage and at 0% all main fuel flow goes to the airblast main-2 stage. Note that center and the right columns cover the same frequency range but with different y-axis scaling; the y-axis scaling is 10× greater in the right column.

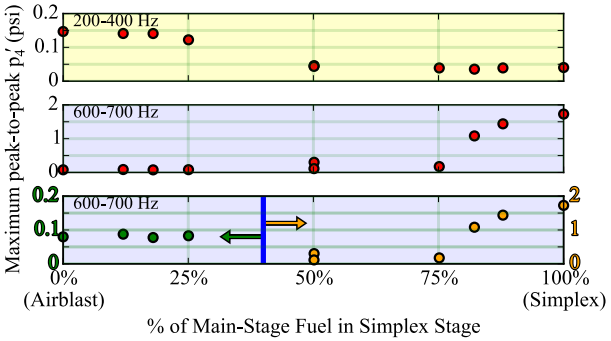

Figure 8. Maximum peak-to-peak dynamic pressure fluctuation p'_4 in different frequency ranges. Note that the middle and bottom graphs plot the same data, with the only difference being the $y-$axis scale. The y-axis scale for the middle graph is 10× that of the top graph. The y-axis scale for the left side of the bottom plot is the same as that of the top plot and for the right side is the same as that of the middle plot.

peak dynamic pressure fluctuations was identified at an inlet temperature of 450°F, a pressure of 100 psia, an air pressure drop of 3%, and an overall equivalence ratio of 0.35. The high combustion dynamics were found with only the pilot and the simplex main-1 stage fueled. These dynamic pressure fluctuations could be reduced to below 0.5 psi by shifting half of the main-stage fuel flow from the simplex main-1 stage to the airblast main-2 stage. In addition to reducing combustion dynamics, this fuel-shift decreases NO_x emissions. It increases CO and hydrocarbon emissions, but leaves them at levels acceptable for low power operation (>99.5% combustion efficiency). Therefore, to mitigate combustion dynamics and reduce NO_x while keeping combustion efficiency high, future configurations should continue to use both simplex and airblast fuel injectors.

Acknowledgments

The CE-5 crew made this work possible: Jonathan Kubiak, Tom Barkis, Laura Acosta, Alan Revilock, Daniel Washington, Julian Iera, Bill Rozman, and Harold Redloske. Zhuohui He provided research support during testing of the first two configurations.

The development of the N+2 hardware and the testing of the 5-recess and flat dome configurations were supported by NASA's Environmentally Responsible Aviation (ERA) project. The testing of the 9-recess configuration was supported by NASA's Advanced Air Transportation Technologies (AATT) program.

The data was processed using the IPython[28], numpy[29], pandas[30], and matplotlib[31] python pack-

ages.

References

[1] Tacina, R. R., "Low-NOx Potential of Gas Turbine Engines," AIAA-1989-0550, 1989.

[2] Lee, C.-M., Bianco, J., Deur, J., and Ghorashi, B., "Nitric Oxide Formation in a Lean Premixed Prevaporized Jet A/Air Flame Tube: an Experimental and Analytical Study," NASA/TM–2001-105722, 1992.

[3] Tacina, R., Lee, P., and Wey, C., "A Lean-Direct-Injection Combustor Using a 9 Point Swirl-Venturi Fuel Injector," ISABE-2005-1106, 2005.

[4] Tacina, R., Wey, C., Laing, P., and Mansour, A., "A Low-NOx Lean-Direct Injection, MultiPoint Integrated Module Combustor Concept for Advanced Aircraft Gas Turbines," NASA/TM–2002-211347, 2005.

[5] Tacina, R., Mao, C.-P., and Wey, C., "Experimental Investigation of a Multiplex Fuel Injector Module with Discrete Jet Swirlers for Low Emissions Combustors," AIAA-2004-0135, 2004.

[6] Sattinger, S. S., Neumeier, Y., Nabi, A., Zinn, B. T., Amos, D. J., and Darling, D. D., "Sub-Scale Demonstration of the Active Feedback Control of Gas-Turbine Combustion Instabilities," 98-GT-258, 1998.

[7] Lieuwen, T. and McManus, K., "Introduction: Combustion Dynamics in Lean-Premixed Prevaporized (LPP) Gas Turbines," *Journal of Propulsion and Power*, Vol. 19, No. 5, 2003.

[8] Huang, Y. and Yang, V., "Dynamics and stability of lean-premixed swirl-stabilized combustion," *Progress in Energy and Combustion Science*, Vol. 35, 2009, pp. 293–364.

[9] DeLaat, J. C. and Paxson, D. E., "Charatterization and Simulation of the Thermoacoustic Instability Behavior of an Advanced, Low Emissions Combustor Prototype," AIAA 2008-4878, 2008.

[10] Huang, C., Gejji, R., and Anderson, W. E., "Combustion Dynamics Behavior in a Single-Element Lean Direct Injection (LDI) Gas Turbine Combustor," AIAA 2014-3433, 2014.

[11] Lieuwen, T. C., *Unsteady Combustor Physics*, Cambridge University Press, Cambridge, 1st ed., 2013.

[12] Candel, S., Durox, D., Schuller, T., Brourgouin, J.-F., and Mocek, J. P., "Dynamics of Swirling Flames," *Annual Review of Fluid Mechanics*, Vol. 46, 2014, pp. 147–173.

[13] Ducruix, S., Schuller, T., Durox, D., and Candel, S., "Combustion Dynamics and Instabilities: Elementary Coupling and Driving Mechanisms," *Journal of Propulsion and Power*, Vol. 19, No. 5, 2003.

[14] Beer, J. and Chigier, N., *Combustion Aerodynamics*, John Wiley & Sons, Inc., New York, 1st ed., 1971 1971.

[15] Lefebvre, A. H., *Gas Turbine Combustion*, Taylor and Francis, Philadelphia, 2nd ed., 1998.

[16] Syred, N., "A review of oscillation mechanisms and the role of the precessing vortex core (PVC) in swirl combustion systems," *Progress in Energy and Combustion Science*, Vol. 32, 2006, pp. 93–161.

[17] Heath, C. M., Hicks, Y. R., Anderson, R. C., and Locke, R. J., "Optical Characterization of a Multipoint Lean Direct Injector for Gas Turbine Combustors :Velocity and Fuel Drop Size Measurements," GT2010-22960, 2010.

[18] Hicks, Y. R., Heath, C. M., Anderson, R. C., and Tacina, K. M., "Investigations of a combustor using a 9-point swirl-venturi fuel injector: recent experimental results." ISABE-2011-1106, 2011.

[19] SAE E-31 Technical Committee, "Procedure for the Continuous Sampling and Measurement of Gaseous Emissions from Aircraft Turbine Engines," SAE ARP 1256D, 2011.

[20] SAE E-31 Technical Committee, "Procedure for the Analysis and Evaluation of Gaseous Emissions from Aircraft Engines," SAE ARP 1533B, 2013.

[21] McBride, B. and Gordon, S., "Computer Program for Calculating and Fitting Thermodynamic Functions," NASA RP-1271, 1992.

[22] McBride, B., Zehe, M., and Gordon, S., "NASA Glenn Coefficients for Calculating Thermodynamic Properties of Individual Species," NASA TP-3287, 1993.

[23] Iberall, A. S., "Attenuation of Oscillatory Pressures in Instrument Lines," U.S. Department of Commerce, National Bureau of Standards, Research Paper RP2115, 1950.

[24] Bergh, H. and Tijdeman, H., "Theoretical and Experimental Results for the Dynamic Response of Pressure Measuring Systems," Report NLR-TR F.238, National Aerospace Laboratory, NLR, The Netherlards, 1965.

[25] Samuelson, R., "Pneumatic Instrumentation Lines and their Use in Measuring Rocket Nozzle Pressure," Report No. NR-DR-0124, Aerojet-General Corporation, 1969.

[26] Tacina, K. M., Lee, P., Mongia, H., Chang, C. T., He, Z., and Dam, B., "A Second Generation Swirl-Venturi Lean Direct Injection Combustion Concept," AIAA 2014-3434, 2014.

[27] Ajmani, K., Mongia, H., and Lee, P., "CFD Computations of Emissions For LDI-2 Combustors with Simplex and Airblast Injectors," AIAA 2014-3529, 2014.

[28] Pérez, F. and Granger, B. E., "IPython: a System for Interactive Scientific Computing," *Computing in Science and Engineering*, Vol. 9, No. 3, May 2007, pp. 21–29.

[29] Walt, S. v. d., Colbert, S. C., and Varoquaux, G., "The NumPy Array: A Structure for Efficient Numerical Computation," *Computing in Science and Engineering*, Vol. 13, No. 2, 2011, pp. 22–30.

[30] McKinney, W., "Data Structures for Statistical Computing in Python," *Proceedings of the 9th Python in Science Conference*, edited by S. van der Walt and J. Millman, 2010, pp. 51 – 56.

[31] Hunter, J. D., "Matplotlib: A 2D graphics environment," *Computing In Science & Engineering*, Vol. 9, No. 3, 2007, pp. 90–95.